Rotation-perturbed surface acoustic waves propagating in piezoelectric crystals

Huiyu Fang[a], Jiashi Yang[a], Qing Jiang[b,*]

[a]*Department of Engineering Mechanics, University of Nebraska, Lincoln, NE 68588, USA*
[b]*Department of Mechanical Engineering, University of California, Riverside, CA 92521, USA*

Abstract

This paper represents an analysis of surface acoustic waves propagating in rotating piezoelectric solids. The analysis shows that a piezoelectric material may not permit propagation of more than one rotation-perturbed surface wave even if both the Rayleigh wave and the Bleustein–Gulyaev wave are permissible under a non-rotating condition. © 2000 Elsevier Science Ltd. All rights reserved.

Keywords: Surface acoustic wave; Piezoelectric crystal; Gyroscope

1. Introduction

Piezoelectric crystals have been used to fabricate rotation rate sensors for various applications (see Gates, 1968; Söderkvist, 1994) for review and general discussion. A typical piezoelectric rotation rate sensor utilizes the phenomenon that vibrating a rotating body induces a secondary vibration due to the presence of the Coriolis force and the centrifugal force and the magnitude of the secondary vibration depends on the rotation rate. There have been many developments on designing rotation rate sensors utilizing various vibration modes of piezoelectric structures, including flexural vibrations of beams (Söderkvist, 1991; Chou et al., 1991), torsional and radial vibrations of circular cylindrical shells (Yang, 1997), and thickness-shear vibrations of plates (Reese et al., 1989; Yong et al., 1995; Yang, 1996). These vibrating rotation rate sensors are, however, not suitable for applications that involve high level of shock or impact, because vibrating parts and their connections are fragile. It is known that surface acoustic waves in elastic solids (Wren and Burdess, 1987; Clarke and Burdess, 1994) are disturbed by

---

* Corresponding author. Fax: + 1-909-787-3188.
  E-mail address: qjiang@engr.ucr.edu (Q. Jiang).

H. Fang et al. / International Journal of Solids and Structures 37 (2000) 4933–4947

rotation and that the speeds of the disturbed waves are dependent of rotation rate. This suggests the possibility to design rotation rate sensors based on surface acoustic waves. The present paper presents our analysis of surface acoustic waves propagating in rotating piezoelectric crystals.

In the next section, we present a formulation that governs surface acoustic waves propagating in a rotating piezoelectric solid, including the effects of both the Coriolis force and the centrifugal force. For simplicity, we consider the case that the piezoelectric body rotates about the axis along which the surface acoustic waves propagate. Our analysis presented in Section 3 shows that the rotation-perturbed surface acoustic waves in piezoelectric solids are generally dispersive, even when propagating in a half space. We then reduce the formulation to an eigenvalue problem for determination of the dependence of the wave speed upon the rotation rate. The numerical analysis given in Section 4 leads to only one solution for our model material: PZT-5H, and for two exclusive boundary conditions, i.e., the electroded boundary and the charge-free boundary. It is known that surface wave solutions for non-rotating piezoelectric solids may not be unique (Lothe and Barnett, 1976). There are generally two surface wave solutions, one called the Rayleigh wave because of its resemblance to the Rayleigh wave in elasticity (Rayleigh, 1885), and the other referred to as the Bleustein–Gulyaev wave owing to the original work of Bleustein (1968) and Gulyaev (1969). The former is confined in a plane, called the sagittal plane, and the latter has only one non-zero displacement component that is perpendicular to the sagittal plane. Our solution for PZT-5H has three displacement components and the components within the sagittal plane are substantially larger than the out-of-plane component. Also, the wave speed of this solution approaches to the Rayleigh wave speed as the rotation rate diminishes. We, hence, recognize it as the rotation-perturbed Rayleigh wave. Our numerical results indicate that the wave speed decreases with increasing rotation rate and this dependence appears to be stronger with the electric charge-free boundary condition than with the electroded boundary condition. It is evident from our formulation that the coupling of the in-plane components with the out-of-plane component is due to the presence of the Coriolis force and the centrifugal force. Our further analysis suggests that a rotation-perturbed surface acoustic wave should be slower than the bulk waves of the material, i.e., the longitudinal wave and the shear waves, both the in-plane shear wave and the out-of-plane shear wave. The material properties given by Tiersten (1969) indicate that the Bleustein–Gulyaev wave is faster than the in-plane shear wave for PZT-5H, and hence, we do not expect to find the rotation-perturbed Bleustein–Gulyaev wave for this material. On the other hand, the Rayleigh wave and the Bleustein–Gulyaev wave are both slower than the bulk waves propagating in PZT-6B, and our numerical scheme indeed leads to two solutions, i.e., the rotation-perturbed Rayleigh wave and the rotation-perturbed Bleustein–Gulyaev wave. Finally, we note from our numerical results the quadratic dependence of the reciprocal velocity on the rotation rate, and we recognize that a linear dependence would have been more desirable for sensing applications. In studying other cases, we find that this dependence is nearly linear in the case that the piezoelectric body rotates about an axis that is perpendicular to the propagation direction of surface waves and that is parallel to the material poling direction. We note, however, that one can only find the perturbed Rayleigh wave in this setting because the Bleustein–Gulyaev wave is not affected by rotation.

2. Surface acoustic waves propagating in a rotating piezoelectric crystal

We consider a linear piezoelectric body that occupies the half space, denoted by $x_2 \leq 0$ in the Cartesian frame shown in Fig. 1, and that rotates at a constant rate Ω about the x_1 axis. In the frame that rotates with the body, the equations of motion and Coulomb's law have the following representation:

$$\nabla \cdot \mathbf{T} - 2\rho\Omega\boldsymbol{\zeta} \times \dot{\mathbf{u}} - \rho\Omega^2\boldsymbol{\zeta} \times (\boldsymbol{\zeta} \times \mathbf{u}) = \rho\ddot{\mathbf{u}}, \tag{2.1}$$

$$\nabla \cdot \mathbf{D} = 0, \tag{2.2}$$

where we denote, by $\mathbf{T}$, $\mathbf{u}$, $\mathbf{D}$ and ρ, the stress tensor, the displacement vector, the dielectric displacement vector and the mass density, respectively. ζ stands for the unit vector along the x_1 axis. A superimposed dot indicates differentiation with respect to the time parameter t, and the symbol $\nabla\cdot$ represents divergence with respect to the spatial coordinates $\mathbf{x}$. Note that we have neglected both body forces and body charges for simplicity.

We now recall the linear constitutive relations for piezoelectric solids as follows:

$$\mathbf{T} = \mathbf{cS} - \mathbf{eE}, \tag{2.3}$$

$$\mathbf{D} = \mathbf{e}^{\mathrm{T}}\mathbf{S} + \boldsymbol{\epsilon}\mathbf{E}, \tag{2.4}$$

where $\mathbf{c}$, $\mathbf{e}$ and $\boldsymbol{\epsilon}$ are, respectively, the elasticity tensor, the piezoelectric tensor and the dielectric tensor. A superimposed T indicates transpose. The strain tensor $\mathbf{S}$ and the electric field intensity vector $\mathbf{E}$ are related to the displacement vector $\mathbf{u}$ and the electric potential ϕ through the following:

$$\mathbf{S} = \frac{\nabla\mathbf{u} + (\nabla\mathbf{u})^{\mathrm{T}}}{2}, \qquad \mathbf{E} = -\nabla\phi. \tag{2.5}$$

In the above equation, the symbol ∇ indicates gradient.

We are interested in waves propagating along a surface free of mechanical loads, i.e.

$$\mathbf{Tn} = \mathbf{0}, \qquad x_2 = 0, \tag{2.6}$$

where $\mathbf{n}$ denotes the unit vector along the x_2 axis. There are usually three exclusive cases of electric boundary conditions associated with a free surface. The first corresponds to an electroded surface, i.e.

$$\phi = 0, \qquad x_2 = 0; \tag{2.7}$$

the second represents a charge-free surface, i.e.

$$\mathbf{D} \cdot \mathbf{n} = 0, \qquad x_2 = 0, \tag{2.8}$$

and the third takes into account the effect of solid/air interface by requiring continuity of both the electric potential and the normal component of the dielectric displacement across the interface. For simplicity, we restrict our analysis to the first two cases. Furthermore, we require that both the
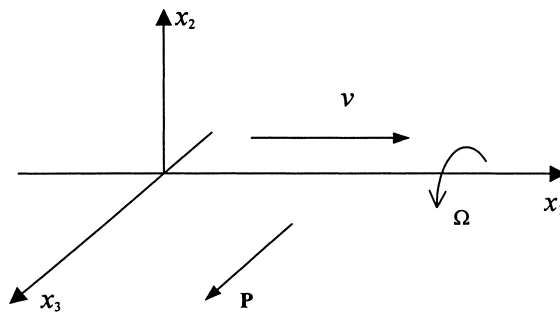

Fig. 1. A surface wave propagating along the x_1 direction in a piezoelectric half-space which is poled along the x_3 direction and rotates about the x_1 axis.

displacement and the electric potential diminish with depth because of our interest in surface waves, i.e.

$$\lim_{x_2 \to -\infty} \mathbf{u} = \mathbf{0}, \qquad \lim_{x_2 \to -\infty} \phi = 0, \tag{2.9}$$

Considering a surface wave propagating along the x_1 direction, we seek solutions of the following form:

$$\mathbf{u}(\mathbf{x}, t) = \mathbf{a}(x_2)e^{i(kx_1 - \omega t)}, \qquad \phi(\mathbf{x}, t) = a_4(x_2)e^{i(kx_1 - \omega t)}, \tag{2.10}$$

where k and ω are, respectively, the wave number and the frequency.

We consider piezoelectric crystals of a tetragonal system with point group 4 mm, and we note that polycrystalline ferroelectric ceramics are of the same symmetry. Placing the x_3 axis along the four-fold axis and using the compressed matrix notation (Tiersten, 1969), we represent the elasticity tensor, the piezoelectric tensor and the dielectric tensor by the following matrices:

$$\begin{pmatrix} c_{11} & c_{12} & c_{13} & 0 & 0 & 0 \\ c_{12} & c_{11} & c_{13} & 0 & 0 & 0 \\ c_{13} & c_{13} & c_{33} & 0 & 0 & 0 \\ 0 & 0 & 0 & c_{44} & 0 & 0 \\ 0 & 0 & 0 & 0 & c_{44} & 0 \\ 0 & 0 & 0 & 0 & 0 & c_{66} \end{pmatrix}, \begin{pmatrix} 0 & 0 & e_{31} \\ 0 & 0 & e_{31} \\ 0 & 0 & e_{33} \\ 0 & e_{15} & 0 \\ e_{15} & 0 & 0 \\ 0 & 0 & 0 \end{pmatrix}, \begin{pmatrix} \epsilon_{11} & 0 & 0 \\ 0 & \epsilon_{11} & 0 \\ 0 & 0 & \epsilon_{33} \end{pmatrix}, \tag{2.11}$$

where $c_{66} = (c_{11} - c_{12})/2$. In this case, the equation of motion (2.1) and Coulomb's law (2.2) take the following form:

$$c_{11}u_{1, 11} + c_{12}u_{2, 21} + c_{66}(u_{1, 22} + u_{2, 12}) = \rho \ddot{u}_1,$$

$$c_{66}(u_{1, 21} + u_{2, 11}) + c_{12}u_{1, 12} + c_{11}u_{2, 22} = \rho \ddot{u}_2 - 2\rho\Omega \dot{u}_3 - \rho\Omega^2 u_2,$$

$$\bar{c}_{44}(u_{3, 11} + u_{3, 22}) = \rho \ddot{u}_3 + 2\rho\Omega \dot{u}_2 - \rho\Omega^2 u_3,$$

$$\psi_{,11} + \psi_{,22} = 0 \tag{2.12}$$

where

$$\psi = \phi - \frac{e_{15}}{\epsilon_{11}}u_3, \qquad \bar{c}_{44} = c_{44} + \frac{e_{15}^2}{\epsilon_{11}}. \tag{2.13}$$

Please note that material homogeneity is assumed in this analysis.

3. Perturbed surface acoustic waves

In the present section, we seek solutions of Eq. (2.12) of form given by Eq. (2.10) that satisfy the mechanical boundary conditions (2.6), the electric boundary condition either (2.7) or (2.8), and the surface wave conditions (2.9). To seek solutions that decay exponentially with depth, we assume that

$$u_1(\mathbf{x}, t) = A_1 e^{k\eta x_2}e^{i(kx_1 - \omega t)}, \qquad u_2(\mathbf{x}, t) = iA_2 e^{k\eta x_2}e^{i(kx_1 - \omega t)},$$

$$u_3(\mathbf{x}, t) = A_3 e^{k\eta x_2} e^{i(kx_1 - \omega t)}, \qquad \psi(\mathbf{x}, t) = A_4 e^{kx_2} e^{i(kx_1 - \omega t)}, \tag{3.1}$$

and we require that η and k are both positive. We now turn to determine the wave number k, the decaying rate η (scaled by the wave number, for convenience), and the relations among the displacement magnitudes A_1, A_2, A_3 and the electric potential magnitude A_4. We note that ψ given by Eq. (3.1)$_4$ satisfies Eq. (2.12)$_4$. Requiring that the displacements given in Eq. (3.1) satisfy the equations of motions results in a system of linear homogeneous equations for the displacement magnitudes A_1, A_2, A_3 with the following coefficient matrix:

$$\begin{pmatrix} (c_{66}\eta^2 - c_{11})k^2 + \rho\omega^2 & -(c_{12} + c_{66})\eta k^2 & 0 \\ (c_{12} + c_{66})\eta k^2 & (c_{11}\eta^2 - c_{66})k^2 + \rho\omega^2 + \rho\Omega^2 & -2\rho\Omega\omega \\ 0 & -2\rho\Omega\omega & \bar{c}_{44}(\eta^2 - 1)k^2 + \rho\omega^2 + \rho\Omega^2 \end{pmatrix} \tag{3.2}$$

This represents an eigenvalue problem. For nontrivial solutions, the determinant of the coefficient matrix must vanish and this leads to

$$\left[c_{11}(\eta^2 - 1)/(\rho V^2) + 1\right]\left[c_{66}(\eta^2 - 1)/(\rho V^2) + 1\right]\left[\bar{c}_{44}(\eta^2 - 1)/(\rho V^2) + 1\right]$$

$$= \left[(c_{66}\eta^2 - c_{11})/(\rho V^2) + 1\right](c_{11} - c_{66})^2\eta^2/(\rho^2 V^4)](\Omega/\omega)^2$$

$$- \left[(c_{66}\eta^2 - c_{11})/(\rho V^2) + 1\right]\left[(c_{11}\eta^2 + \bar{c}_{44}\eta^2 - c_{66} - \bar{c}_{44})/(\rho V^2) - 2\right](\Omega/\omega)^2$$

$$- \left[(c_{66}\eta^2 - c_{11})/(\rho V^2) + 1\right](\Omega/\omega)^4. \tag{3.3}$$

To obtain the above, we have used the relation: $k = \omega/V$, where V denotes the surface acoustic wave speed. This relation indicates that the wave speed V generally depends upon the frequency ω, i.e., the perturbed surface acoustic wave is dispersive.[1] For convenience of later discussion, we rewrite Eq. (3.3) as

$$\left[(\eta^2 - 1)(V_1/V)^2 + 1\right]\left[(\eta^2 - 1)(V_2/V)^2 + 1\right]\left[(\eta^2 - 1)(V_3/V)^2 + 1\right]$$

$$= \eta^2\left[\eta^2(V_2/V)^2 - (V_1/V)^2 + 1\right]\left[(V_1/V)^2 - (V_2/V)^2\right]^2(\Omega/\omega)^2$$

$$- \left[\eta^2(V_2/V)^2 - (V_1/V)^2 + 1\right]\left[\eta^2(V_1/V)^2 - (V_2/V)^2 + (\eta^2 - 1)(V_3/V)^2 - 2\right](\Omega/\omega)^2$$

$$- \left[\eta^2(V_2/V)^2 - (V_1/V)^2 + 1\right](\Omega/\omega)^4 \tag{3.4}$$

where

$$V_1 = \sqrt{\frac{c_{11}}{\rho}}, \quad V_2 = \sqrt{\frac{c_{66}}{\rho}}, \quad V_3 = \sqrt{\frac{\bar{c}_{44}}{\rho}}. \tag{3.5}$$

---

[1] We acknowledge one of the reviewers for noting the mistake we made in a previous version by neglecting the effect of the centrifugal force.

We note that V_1 is the longitudinal wave speed propagating along the x_1 direction and that V_2 and V_3 are the speeds of shear waves propagating along the x_1 direction with particles moving, respectively, along the x_2 direction and the x_3 direction.

We need to determine the eigenvalues η by solving Eq. (3.4) with the unknown wave speed V and to obtain the corresponding eigenvectors $\mathbf{A}$ from Eq. (3.2). To satisfy three mechanical boundary conditions given by (2.6) and one electric boundary condition given by either (2.7) or (2.8), one generally needs three independent eigenvectors. This requires that the dispersion relation (3.4) have three roots for η^2 which must be positive in order to satisfy the surface wave conditions (2.9). We have not found general conditions under which Eq. (3.4) has three positive roots. At this point, we assume that it has three distinct positive roots and we verify this assumption in our numerical analysis for specific model materials. We denote, by η_m and $\mathbf{A}^{(m)}$, the corresponding positive eigenvalues and eigenvectors, and we thus obtain the following representation for the displacement and the electric potential:

$$u_1 = \sum_{m=1}^{3} C_m \bar{A}_1^{(m)} e^{k\eta_m x_2} e^{i(kx_1 - \omega t)},$$

$$u_2 = \sum_{m=1}^{3} i C_m \bar{A}_2^{(m)} e^{k\eta_m x_2} e^{i(kx_1 - \omega t)},$$

$$u_3 = \sum_{m=1}^{3} C_m \bar{A}_3^{(m)} e^{k\eta_m x_2} e^{i(kx_1 - \omega t)},$$

$$\psi = C_4 e^{kx_2} e^{i(kx_1 - \omega t)}, \tag{3.6}$$

where $\bar{\mathbf{A}}^{(m)}$, $m = 1, 2, 3$, are the scaled eigenvectors defined as:

$$\bar{A}_1^{(m)} = A_1^{(m)} / A_2^{(m)} = \eta_m \big[(V_1/V)^2 - (V_2/V)^2 \big] / \big[\eta_m^2 (V_2/V)^2 - (V_1/V)^2 + 1 \big],$$

$$\bar{A}_2^{(m)} = A_2^{(m)} / A_2^{(m)} = 1,$$

$$\bar{A}_3^{(m)} = A_3^{(m)} / A_2^{(m)} = 2(\Omega/\omega) / \Big[(\eta_m^2 - 1)(V_3/V)^2 + 1 + (\Omega/\omega)^2 \Big]. \tag{3.7}$$

For convenience, we set in Eq. (3.6) $C_m = A_2^{(m)}$ and $C_4 = A_4$. The displacement and the electric potential presented in Eq. (3.6) contain four unknown magnitudes C_j, $j = 1, 2, 3, 4$, and the unknown wave speed V. Requiring that Eq. (3.6) satisfy the mechanical boundary conditions (2.6) and the electric boundary condition either (2.7) or (2.8) leads to determination of the wave speed and the relations among the magnitudes.

In the case that the traction-free surface is electroded, substitution of Eq. (3.6) into Eqs. (2.6) and (2.7) leads to a system of four linear homogeneous equations for the unknown magnitudes C_j, $j = 1, 2, 3, 4$. For nontrivial solutions, we require that the determinant of the coefficient matrix vanish, i.e.

$$\det \begin{pmatrix} \bar{A}_1^{(1)}\eta_1 - \bar{A}_2^{(1)} & \bar{A}_1^{(2)}\eta_2 - \bar{A}_2^{(2)} & \bar{A}_1^{(3)}\eta_3 - \bar{A}_2^{(3)} & 0 \\ c_{12}\bar{A}_1^{(1)} + c_{11}\bar{A}_2^{(1)}\eta_1 & c_{12}\bar{A}_1^{(2)} + c_{11}\bar{A}_2^{(2)}\eta_2 & c_{12}\bar{A}_1^{(3)} + c_{11}\bar{A}_2^{(3)}\eta_3 & 0 \\ \bar{c}_{44}\bar{A}_3^1\eta_1 & \bar{c}_{44}\bar{A}_3^2\eta_2 & \bar{c}_{44}\bar{A}_3^3\eta_3 & e_{15} \\ e_{15}\bar{A}_3^{(1)} & e_{15}\bar{A}_3^{(1)} & e_{15}\bar{A}_3^{(1)} & \epsilon_{11} \end{pmatrix} = 0. \tag{3.8}$$

In the next section, we solve Eq. (3.8) numerically to determine the wave speed V.

In the case that the traction-free surface is also charge-free, the electric boundary condition (2.8) requires that the potential ψ vanish identically and this, together with Eq. (2.13)$_1$, implies that the electric potential ϕ is proportional to the displacement u_3. Substitution of the three displacements given by Eq. (3.6) into the mechanical boundary conditions Eq. (2.6) yields a system of three linear homogeneous equations for the displacement magnitudes A_m, $m = 1, 2, 3$. Requiring that the system have nontrivial solutions leads to the following equation to determine the wave speed:

$$\det \begin{pmatrix} \bar{A}_1^{(1)}\eta_1 - \bar{A}_2^{(1)} & \bar{A}_1^{(2)}\eta_2 - \bar{A}_2^{(2)} & \bar{A}_1^{(3)}\eta_3 - \bar{A}_2^{(3)} \\ c_{12}\bar{A}_1^{(1)} + c_{11}\bar{A}_2^{(1)}\eta_1 & c_{12}\bar{A}_1^{(2)} + c_{11}\bar{A}_2^{(2)}\eta_2 & c_{12}\bar{A}_1^{(3)} + c_{11}\bar{A}_2^{(3)}\eta_3 \\ \bar{c}_{44}\bar{A}_3^1\eta_1 & \bar{c}_{44}\bar{A}_3^2\eta_2 & \bar{c}_{44}\bar{A}_3^3\eta_3 \end{pmatrix} = 0. \tag{3.9}$$

4. Determination of the wave speed

We are primarily interested in the effect of rotation on the surface acoustic wave speed. To solve Eqs. (3.8) and (3.9) numerically, we use PZT-5H as a model material whose material parameters are given in the book of Tiersten (1969) and are listed in Table 1. To plot the dependence of the surface acoustic wave speed V upon the rotation rate Ω, we find it is convenient to introduce the following dimensionless parameters:

$$X = \left(\frac{\Omega}{\omega}\right)^2, \qquad Y = \frac{V_1}{V}. \tag{4.1}$$

We have plotted Y vs. X in Figs. 2 and 3, respectively, for the electroded surface and the charge-free surface. The results show that the wave speed decreases with increasing rotation rate. A comparison of Figs. 2 and 3 suggests that the rotation effect on the wave speed is stronger when the traction-free surface is electroded instead of charge-free.

Table 1
Material properties

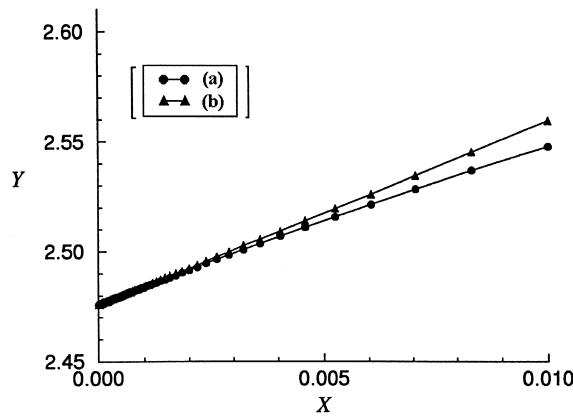| Material	ρ	c_{11}	c_{44}	c_{66}	e_{15}	ε_{11}	$\bar{c}_{44}$
PZT-5H	7500	12.6	2.30	2.325	17.0	1.505	4.220
PZT-5A	7750	12.1	2.11	2.257	12.3	0.811	3.975
PZT-6B	7550	16.8	3.55	4.167	4.6	0.360	4.134
BaTiO$_3$	5700	15.0	4.39	4.237	11.4	0.987	5.707

Fig. 2. Variations of the speed of the rotation-perturbed Rayleigh wave for PZT-5H; the traction-free surface is electroded: (a) with the eigenvalues determined from Eq. (3.3); (b) with the approximated eigenvalues given by Eq. (4.5).

Note that the elastic moduli, the piezoelectric coefficient, the dielectric constant and the mass density in Table 1 are given in 10^{10} N/m^2, C/m^2, 10^{-8} C/V m and kg/m^3, respectively.

It is known that surface wave solutions for non-rotating piezoelectric solids may not be unique. There may be two surface wave solutions, i.e., the Rayleigh wave and the Bleustein–Gulyaev wave. Our numerical analysis, however, delivers only one solution for PZT-5H and the wave speed of this solution approaches the Rayleigh wave speed as the rotation rate diminishes. For further understanding of this issue, we reduce our formulation to the non-rotating case: $\Omega = 0$. Without rotation, Eqs. (3.2) and (3.3), or (3.4) equivalently, reduce to

$$\begin{pmatrix} \left(c_{66}\eta^2 - c_{11}\right) + \rho V^2 & -(c_{12} + c_{66})\eta & 0 \\ (c_{12} + c_{66})\eta & \left(c_{11}\eta^2 - c_{66}\right) + \rho V^2 & 0 \\ 0 & 0 & \bar{c}_{44}\left(\eta^2 - 1\right) + \rho V^2 \end{pmatrix} \begin{pmatrix} A_1 \\ A_2 \\ A_3 \end{pmatrix} = \begin{pmatrix} 0 \\ 0 \\ 0 \end{pmatrix}, \qquad (4.2)$$
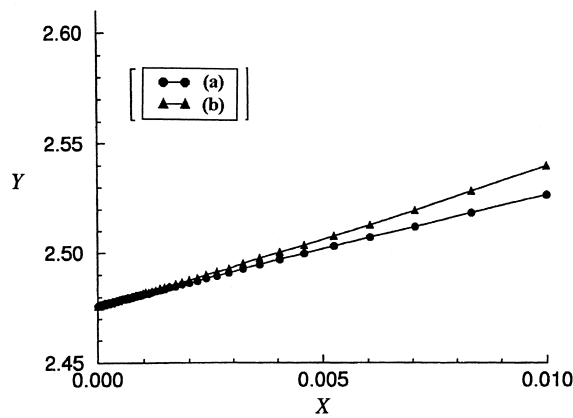

Fig. 3. Variations of the speed of the rotation-perturbed Rayleigh wave for PZT-5H; the traction-free surface is free of electric charges: (a) with the eigenvalues determined from Eq. (3.3); (b) with the approximated eigenvalues given by Eq. (4.5).

and

$$\left[(\eta^2 - 1)(V_1/V)^2 + 1\right]\left[(\eta^2 - 1)(V_2/V)^2 + 1\right]\left[(\eta^2 - 1)(V_3/V)^2 + 1\right]\big] = 0. \tag{4.3}$$

From Eq. (4.3), one can readily determine the eigenvalues:

$$\bar{\eta}_1 = \sqrt{1 - (V/V_1)^2}, \qquad \bar{\eta}_2 = \sqrt{1 - (V/V_2)^2}, \qquad \bar{\eta}_3 = \sqrt{1 - (V/V_3)^2}. \tag{4.4}$$

Note from Eq. (4.2) that A_1 and A_2 are decoupled from A_3. Taking the eigenvalues $\bar{\eta}_1$, $\bar{\eta}_2$, and setting $A_3 = 0$, one may obtain a surface wave with particles moving in the sagittal plane ($x_3 = 0$), i.e., the Rayleigh wave. For the eigenvalues $\bar{\eta}_1$ and $\bar{\eta}_2$ to be real, the Rayleigh wave speed V_R must be smaller than both the longitudinal wave speed V_1 and the shear wave speed V_2. Using the third eigenvalue $\bar{\eta}_3$ and taking $A_1 = A_2 = 0$ may lead to a surface wave with particles moving perpendicular to the sagittal plane, that is, the Bleustein–Gulyaev wave. We denote by V_B the Bleustein–Gulyaev wave speed, and we note that V_B is always lower than the shear wave speed V_3.

In view of Eq. (3.4), we expect that the eigenvalues η_m^2, $m = 1, 2, 3$ differ slightly from their non-rotation values $\bar{\eta}_m^2$ when the ratio Ω/ω is small, and hence, we approximate the eigenvalues η_m^2 by $\hat{\eta}_m^2 = \bar{\eta}_m^2 + \Delta_m(\Omega/\omega)^2$, $m = 1, 2, 3$. Thus, the sign of the eigenvalue $\hat{\eta}_m^2$ is determined by that of $\bar{\eta}_m^2$ when $(\Omega/\omega)^2$ is sufficiently small except that $\bar{\eta}_m^2$ vanishes. We note that the exception case corresponds to leaky waves, instead of surface waves. As discussed previously, there may exist a surface wave only if the three eigenvalues η_m^2 are all positive. Together with Eq. (4.4), this indicates that the surface acoustic wave speed of a rotating piezoelectric body should generally be smaller than the longitudinal wave speed V_1 and the shear wave speeds both V_2 and V_3. Hence, we do not expect to find a surface wave that corresponds to the Bleustein–Gulyaev wave if the Bleustein–Gulyaev wave speed is larger than any of the bulk wave speeds V_1, V_2 and V_3. For PZT-5H, we have the relations: $V_R < V_2 < V_B < V_3 < V_1$, as shown in Table 2, and therefore, we should not expect to find the disturbed Bleustein–Gulyaev wave by rotation. In Table 2, we also list the wave speeds for PZT-5A, PZT-6B and barium titanate, according to Jaffe and Berlincourt (1965). As one can see from Table 1, PZT-6B is the only material among those listed in Table 2 whose Bleustein–Gulyaev wave speed is smaller than all the bulk wave speeds V_1, V_2 and V_3, and hence, we may find the rotation-disturbed Bleustein–Gulyaev wave for PZT-6B. It is known that existence of surface waves depends upon boundary conditions. According to the work of Lothe and Barnett (1976) on surface waves propagating in non-rotating piezoelectric materials, there exists at most one subsonic wave propagating along a surface free of both mechanical loads and electric charges, corresponding to the boundary conditions (2.6) and (2.8). Reducing our formulation to the non-rotating case, one can show that the Bleustein–Gulyaev wave is not permissible by the boundary conditions (2.6) and (2.8). We, therefore, consider the boundary conditions (2.6) and (2.7), corresponding to an electroded surface that is free of mechanical loads, and seek solutions within the range of rotation rate: $0 < X < 0.01$. Please note our assumption that $\sqrt{X} = \Omega/\omega \ll 1$. We find two solutions, one within the

Table 2
Comparison of wave speeds

Material	V_1	V_2	V_3	V_R	V_B	Sorting
PZT-5H	4099	1761	2372	1656	2112	$V_R < V_2 < V_B < V_3 < V_1$
PZT-5A	3951	1707	2265	1645	2000	$V_R < V_2 < V_B < V_3 < V_1$
PZT-6B	4717	2349	2340	2302	2316	$V_R < V_B < V_3 < V_2 < V_1$
BaTiO$_3$	5130	2726	3164	2681	3079	$V_R < V_2 < V_B < V_3 < V_1$

entire range of rotation rate, corresponding to the perturbed Rayleigh wave, and the other only for $X < 6 \times 10^{-5}$, representing the perturbed Bleustein–Gulyaev wave. The numerical results are plotted in Figs. 4 and 5, respectively. To see why our numerical program can not find the second solution for $X > 6 \times 10^{-5}$, we show in Fig. 5 the region (the shaded area) in which Eq. (3.4) has three positive roots for PZT-6B. We see that the solution ends at the boundary of this region where $X \approx 6 \times 10^{-5}$. While, for PZT-5A and barium titanate, we find only one solution corresponding to the Rayleigh wave, and the variations of the wave speed with the rotation rate for these materials are plotted in Fig. 6. As discussed above, we do not expect to find a surface wave that corresponds to the Bleustein–Gulyaev wave for these materials.

Furthermore, miniaturization of such sensors requires that the surface waves in operation be of a wave length no more than a few microns, and correspondingly, the operation frequency ω should significantly higher than the rotation rate Ω of mechanical machinery, typically a few thousand revolutions per minute. Therefore, the ratio Ω/ω should be a small parameter, and this suggests that one may tackle the problem using a perturbation analysis. By approximating the eigenvalues η_m^2 by $\hat{\eta}_m^2 = \bar{\eta}_m^2 + \Delta_m(\Omega/\omega)^2$, $m = 1, 2, 3$, we obtain from Eq. (3.4)

$$\hat{\eta}_1^2 = \bar{\eta}_1^2 + (V/V_1)^2(V/V_2)^2(V/V_3)^2 \frac{F(V, \bar{\eta}_1)}{(\bar{\eta}_1^2 - \bar{\eta}_2^2)(\bar{\eta}_1^2 - \bar{\eta}_3^2)}(\Omega/\omega)^2$$

$$\hat{\eta}_2^2 = \bar{\eta}_2^2 + (V/V_1)^2(V/V_2)^2(V/V_3)^2 \frac{F(V, \bar{\eta}_2)}{(\bar{\eta}_2^2 - \bar{\eta}_3^2)(\bar{\eta}_2^2 - \bar{\eta}_1^2)}(\Omega/\omega)^2$$

$$\hat{\eta}_3^2 = \bar{\eta}_3^2 + (V/V_1)^2(V/V_2)^2(V/V_3)^2 \frac{F(V, \bar{\eta}_3)}{(\bar{\eta}_3^2 - \bar{\eta}_1^2)(\bar{\eta}_3^2 - \bar{\eta}_2^2)}(\Omega/\omega)^2 \tag{4.5}$$

where

$$F(V, \eta) = -\left[\eta^2(V_2/V)^2 - (V_1/V)^2 + 1\right]\left[\eta^2(V_1/V)^2 - (V_2/V)^2 + (\eta^2 - 1)(V_3/V)^2 - 2\right] - \bigg[$$

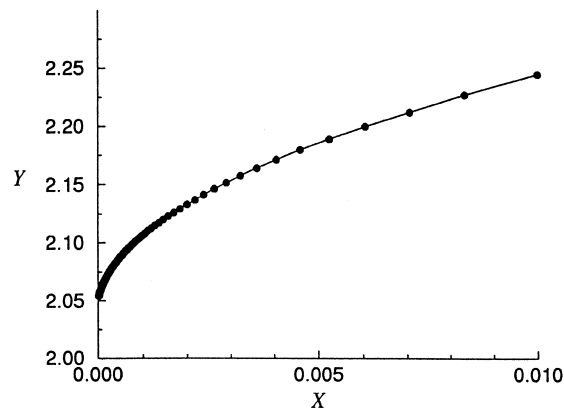$$\times (V_1/V)^2 - (V_2/V)^2\bigg]^2 \eta^2. \tag{4.6}$$

Fig. 4. Variations of the speed of the rotation-perturbed Rayleigh wave for PZT-6B; the traction-free surface is electroded.
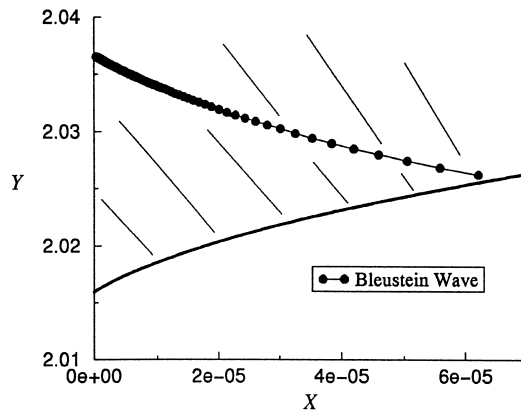
Fig. 5. Variations of the speed of the rotation-perturbed Bleustein–Gulyaev wave for PZT-6B; the traction-free surface is electroded. The shaded area indicates the region in which there are three positive eigenvalues for PZT-6B.

We need to substitute these approximated eigenvalues in Eq. (3.7) to approximate the corresponding eigenvectors. We then have to approximate Eqs. (3.8) and (3.9), respectively, for the electroded and charge-free surfaces, using the approximated eigenvalues and approximated eigenvectors, and finally we should solve the resulting equations for an approximated expression of the surface wave speed. We have to give up this attempt because it is too algebraically involved. We note, however, that it is very time-consuming to search for three positive roots of Eq. (3.4) with the unknown wave speed to be determined by solving either Eq. (3.8) or (3.9), because it usually requires the use of an iterative procedure. As an alternative numerical procedure, we substitute the approximated eigenvalues given in Eq. (4.5) into Eqs. (3.8) and (3.9) to determine the variations of the surface wave speed with rotation rate, respectively, for the electroded surface and the charge-free surface. The results for PZT-5H are plotted, respectively, in Figs. 2 and 3 for comparison with the results obtained from the full solution. The comparison indicates that the approximation is fairly good for $(\Omega/\omega)^2 \leq 0.005$, and that the error becomes increasingly large as the frequency ratio increases.
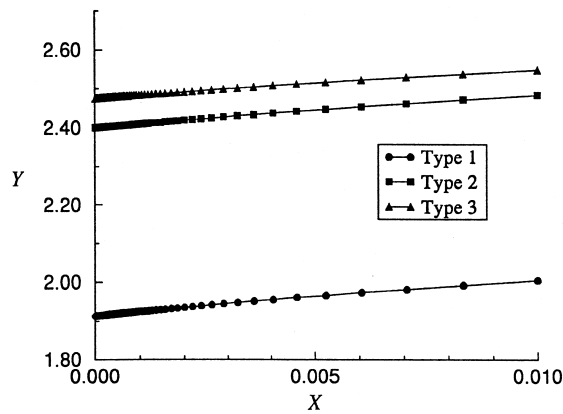

Fig. 6. Variations of the speed of the rotation-perturbed Rayleigh wave for barium titanate (Type 1), PZT-5A (Type 2) and PZT-5H (Type 3); the traction-free surface is electroded.

5. Discussion

The perturbation analysis is helpful for us to understand the suppression of the Bleustein–Gulyaeve wave in PZT-5H by rotation, although it did not lead us to an approximated relation of the surface wave speed with the rotation rate. The perturbed Bleustein–Gulyaeve wave requires that all the three eigenvalues, instead of η_3 alone as in the non-rotating case, be positive because rotation results in coupling of the out-of-plane displacement with the in-plane displacements. The approximated expressions for the eigenvalues given in Eq. (4.5) together with Eq. (4.4) show that all the three eigenvalues are positive only if the Bleustein–Gulyaeve wave speed V_B is lower than all the bulk wave speeds V_1, V_2, and V_3. This requires that $V_B < V_2$ because it is guaranteed that $V_B < V_3$ and $V_2 < V_1$ for all the materials.

We note from the numerical results the quadratic dependence of the reciprocal velocity on the rotation rate, and this suggests that sensors based upon these phenomena will not be very sensitive to low rotation rate, as pointed out to us by one of the reviewers. This has motivated us to examine other cases. We find rotation about the x_3 axis, instead of the x_1 axis, is of some particular interest and we summarize below some of the results. In this case, the equations of motion and the Coulomb's law are given as follows:

$$c_{11}u_{1,\,11} + c_{12}u_{2,\,21} + c_{66}(u_{1,\,22} + u_{2,\,12}) = \rho\ddot{u}_1 - 2\rho\Omega\dot{u}_2 - \rho\Omega^2 u_1,$$

$$c_{66}(u_{1,\,21} + u_{2,\,11}) + c_{12}u_{1,\,12} + c_{11}u_{2,\,22} = \rho\ddot{u}_2 + 2\rho\Omega\dot{u}_1 - \rho\Omega^2 u_2,$$

$$c_{44}(u_{3,\,11} + u_{3,\,22}) + e_{15}(\phi_{,11} + \phi_{,22}) = \rho\ddot{u}_3,$$

$$e_{15}(u_{3,\,11} + u_{3,\,22}) - \epsilon_{11}(\phi_{,11} + \phi_{,22}) = 0, \tag{5.1}$$

The traction-free condition is given as

$$x_2 = 0: \quad \begin{aligned} &c_{12}u_{1,\,1} + c_{11}u_{2,\,2} = 0, \\ &c_{66}(u_{1,\,2} + u_{2,\,1}) = 0, \\ &c_{44}u_{3,\,2} + e_{15}\phi_{,2} = 0 \end{aligned} \tag{5.2}$$

The electroded and charge-free boundary conditions have the following respective representations:

$$x_2 = 0: \quad \phi = 0, \tag{5.3}$$

$$x_2 = 0: \quad e_{15}u_{3,\,2} - \epsilon_{11}\phi_{,2} = 0, \tag{5.4}$$

It is evident from Eqs. (5.1)–(5.4) that rotation does not affect the out-of-plane displacement u_3 and the electrical potential ϕ, and that the third and fourth equations of (5.1) are identical to the equations that, together with the boundary conditions (5.2)$_3$ and (5.4), lead to the Bleustein–Gulyaev wave in the non-rotation case. We, therefore, do not expect the Bleustein–Gulyaev wave to be perturbed by the rotation in the present case. To study the perturbed Rayleigh wave, we are interested in solutions of the first two equations of Eq. (5.1) with the boundary conditions given by the first two equations of Eq. (5.2) that govern the in-plane displacements u_1 and u_2. We note that the first two equations of Eq. (5.1) are decoupled from the third and fourth, and correspondingly, the boundary conditions given in Eqs. (5.2) and (5.4) are decoupled as well. To seek the perturbed Rayleigh wave solution, we set

$$u_1 = A_1 e^{k\eta x_2} e^{i(kx_1 - \omega t)}, \qquad u_2 = iA_2 e^{k\eta x_2} e^{i(kx_1 - \omega t)} \tag{5.5}$$

Substitution from Eq. (5.5) into the first two equations of Eq. (5.1) yields

$$\begin{pmatrix} V_1^2 - V_2^2\eta^2 - V^2[1 + (\Omega/\omega)^2] & (V_1^2 - V_2^2)\eta - 2V^2\Omega/\omega \\ (V_1^2 - V_2^2)\eta + 2V^2\Omega/\omega & V_1^2\eta^2 - V_2^2 + V^2[1 + (\Omega/\omega)^2] \end{pmatrix} \begin{pmatrix} A_1 \\ A_2 \end{pmatrix} = \begin{pmatrix} 0 \\ 0 \end{pmatrix} \tag{5.6}$$

For nontrivial solutions, we require that the determinant of the coefficient matrix in Eq. (5.6) vanish, and this leads to the following characteristic equation:

$$\left[V_1^2\eta^2 - (V_1^2 - V^2) \right]\left[V_2^2\eta^2 - (V_2^2 - V^2) \right]$$

$$= V^2(2V^2 + V_1^2 + V_2^2 - V_1^2\eta^2 - V_2^2\eta^2)(\Omega/\omega)^2 - V^4(\Omega/\omega)^4 \tag{5.7}$$

In the non-rotating case, Eq. (5.7) leads to two distinct positive eigenvalues:

$$\bar{\eta}_1 = \sqrt{1 - (V/V_1)^2}, \qquad \bar{\eta}_2 = \sqrt{1 - (V/V_2)^2}. \tag{5.8}$$

In the case that $\Omega/\omega \ll 1$, we assume that it has two distinct positive eigenvalues η_1 and η_2, and thus obtain the following representation for the in-plane displacements:

$$u_1 = \sum_{m=1}^{2} C_m \bar{A}_1^{(m)} e^{k\eta_m x_2} e^{i(kx_1 - \omega t)},$$

$$u_2 = \sum_{m=1}^{2} iC_m \bar{A}_2^{(m)} e^{k\eta_m x_2} e^{i(kx_1 - \omega t)}, \tag{5.9}$$

where the eigenvectors $\bar{\mathbf{A}}^{(1)}$ and $\bar{\mathbf{A}}^{(2)}$ are defined as

$$\bar{A}_1^{(m)} = (V_1^2 - V_2^2)\eta_m - 2V^2\Omega/\omega, \qquad \bar{A}_2^{(m)} = -V_1^2 + V_2^2\eta_m^2 + V^2[1 + (\Omega/\omega)^2]. \tag{5.10}$$

Substituting Eq. (5.9) into the in-plane traction-free boundary conditions, i.e., the first two of Eq. (5.2), yields

$$\begin{pmatrix} [1 - 2(V_2/V_1)^2]\bar{A}_1^{(1)} + \eta_1\bar{A}_2^{(1)} & [1 - 2(V_2/V_1)^2]\bar{A}_1^{(2)} + \eta_2\bar{A}_2^{(2)} \\ \eta_1\bar{A}_1(1) - \bar{A}_2^{(1)} & \eta_2\bar{A}_1^{(2)} - \bar{A}_2^{(2)} \end{pmatrix} \begin{pmatrix} C_1 \\ C_2 \end{pmatrix} = \begin{pmatrix} 0 \\ 0 \end{pmatrix} \tag{5.11}$$

Requiring that the determinant of the coefficient matrix vanish leads to the following characteristic equation:

$$\left\{ [1 - 2(V_2/V_1)^2]\bar{A}_1^{(1)} + \eta_1\bar{A}_2^{(1)} \right\}\left(\eta_2\bar{A}_1^{(2)} - \bar{A}_2^{(2)} \right)$$

$$= \left\{ [1 - 2(V_2/V_1)^2]\bar{A}_1^{(2)} + \eta_2\bar{A}_2^{(2)} \right\}\left(\eta_1\bar{A}_1^{(1)} - \bar{A}_2^{(1)} \right) \tag{5.12}$$

Substituting Eq. (5.10) into Eq. (5.12) yields

$$\left(1 - V_2^2/V_1^2\right)\left(1 - 2V_2^2/V_1^2\right)\left[-1 + V^2/V_1^2 + \eta_1\eta_2\left(1 - 2V_2^2/V_1^2\right)\right]$$

$$+\left(1 - V_2^2/V_1^2\right)\eta_1\eta_2\left(-1 + V^2/V_1^2 - \eta_1\eta_2 V_2^2/V_1^2\right)$$

$$+\left(-1 + V^2/V_1^2 + \eta_1^2 V_2^2/V_1^2\right)\left(-1 + V^2/V_1^2 + \eta_2^2 V_2^2/V_1^2\right)$$

$$+2(\eta_1 + \eta_2)V^2/V_1^2\left[-\left(1 - 2V_2^2/V_1^2\right)^2 + \eta_1\eta_2 V_2^2/V_1^2\right](\Omega/\omega)$$

$$+V^2/V_1^2\left(1 - 2V_2^2/V_1^2\right)\left(1 - V_2^2/V_1^2 + 4V^2/V_1^2\right)(\Omega/\omega)^2$$

$$+V^2/V_1^2\left[2\left(V^2/V_1^2 - 1\right) + \left(\eta_1^2 + \eta_2^2\right)V_2^2/V_1^2 + \eta_1\eta_2\left(1 - V_2^2/V_1^2\right)\right](\Omega/\omega)^2$$

$$+V^4/V_1^4(\Omega/\omega)^4 = 0 \qquad\qquad\qquad\qquad (5.13)$$

We note that Eq. (5.13) shows the dependence of the Rayleigh wave speed V upon the rotation rate Ω with η_1 and η_2 being the eigenvalues to be determined from Eq. (5.7). The dependence of the Rayleigh wave speed V upon the rotation rate Ω appears to be nearly linear as shown in Fig. 7 for small ratio Ω/ω, and we note that this type of dependence is particularly desirable for sensor applications. Noting Eqs. (5.7) and (5.8), we approximate the eigenvalues as follows:

$$\eta_1 = \bar{\eta}_1 + O\!\left(\frac{\Omega^2}{\omega^2}\right), \qquad \eta_2 = \bar{\eta}_2 + O\!\left(\frac{\Omega^2}{\omega^2}\right). \qquad\qquad (5.14)$$

This together with Eq. (5.13) leads to

$$\left(1 - V_2^2/V_1^2\right)\left(1 - 2V_2^2/V_1^2\right)\left[\left(-1 + V^2/V_1^2\right) + \bar{\eta}_1\bar{\eta}_2\left(1 - 2V_2^2/V_1^2\right)\right]$$
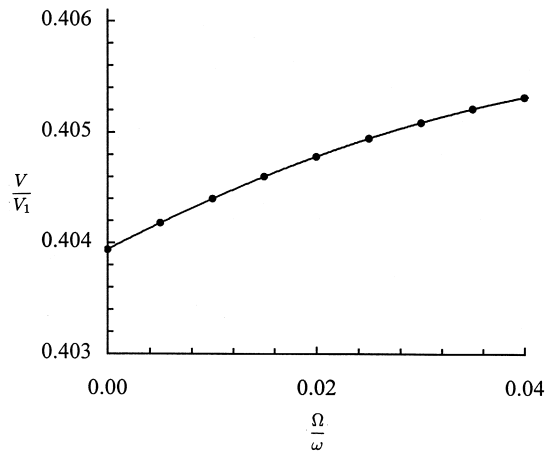

Fig. 7. Variations of the speed of the rotation-perturbed Rayleigh wave for PZT-5H and for rotation about an axis that is perpendicular to the propagation direction of the surface wave and that is parallel to the material poling direction.

$$+\left(1 - V_2^2/V_1^2\right)\bar{\eta}_1\bar{\eta}_2\left(-1 + V^2/V_1^2 - \bar{\eta}_1\bar{\eta}_2 V_2^2/V_1^2\right)$$

$$+\left(-1 + V^2/V_1^2 + \bar{\eta}_1^2 V_2^2/V_1^2\right)\left(-1 + V^2/V_1^2 + \bar{\eta}_2^2 V_2^2/V_1^2\right)$$

$$+2(\bar{\eta}_1 + \bar{\eta}_2)V^2/V_1^2\left[-\left(1 - 2V_2^2/V_1^2\right)^2 + \bar{\eta}_1\bar{\eta}_2 V_2^2/V_1^2\right](\Omega/\omega) + O\left(\Omega^2/\omega^2\right) = 0 \qquad (5.15)$$

The above confirms that the dependence of the Rayleigh wave speed upon the rotation rate is approximately linear for very small ratio Ω/ω.

Acknowledgements

References

Bleustein, J.L., 1968. A new surface wave in piezoelectric materials. Applied Physics Letters 13, 412–413.

Chou, C.S., Yang, J.W., Huang, Y.C., Yang, H.J., 1991. Analysis on vibrating piezoelectric beam gyroscope. International Journal of Applied Electromagnetics and Mechanics 2, 227–241.

Clarke, N.S., Burdess, J.S., 1994. Rayleigh waves on a rotating surface. ASME Journal of Applied Mechanics 61, 724–726.

Gates, W.D., 1968. Vibrating angular rate sensor may threaten the gyroscope. Electronics 41, 103–134.

Gulyaev, Yu.V., 1969. Electroacoustic surface waves in solids. Soviet Physics JETP Letters 9, 37–38.

Jaffe, H., Berlincourt, D.A., 1965. Piezoelectric transducer materials. Proceedings of IEEE 53, 1372–1386.

Lothe, J., Barnett, D.M., 1976. Integral formalism for surface waves in piezoelectric crystals: existence considerations. Journal of Applied Physics 47, 1799–1807.

Rayleigh, L., 1885. On waves propagating along the plane surface of an elastic solid. Proceedings of London Mathematical Society 7, 4–11.

Reese, G.M., Marek, E.L., Lobitz, D.W., 1989. Three dimensional finite element calculations of an experimental quartz rotation sensor. Proceedings of IEEE Ultrasonics Symposium, 419–422.

Söderkvist, J., 1991. Piezoelectric beams and vibrating angular rate sensors. IEEE Transaction of Ultrasonics, Ferroelectrics and Frequency Control 38, 271–280.

Söderkvist, J., 1994. Micromachined gyroscopes. Sensors and Actuators A 43, 65–71.

Tiersten, H.F., 1969. Linear Piezoelectric Plate Vibrations. Plenum Press, New York.

Wren, T., Burdess, J.S., 1987. Surface waves perturbed by rotation. ASME Journal of Applied Mechanics 54, 464–468.

Yang, J.S., 1996. Analysis of ceramic thickness shear piezoelectric gyroscopes. Journal of Acoustical Society of American 102, 3542–3548.

Yang, J.S., 1997. A circular cylindrical shell piezoelectric gyroscope. International Journal of Applied Electromagnetics and Mechanics 8, 259–271.

Yong, Y.-K., Zhang, Z., Hou, J., 1995. On the accuracy of plate theories for prediction of unwanted modes near the fundamental thickness shear mode. Proceedings of IEEE Frequency Control Symposium, 755–760.